Morphology and toughness characterization of epoxy resins modified with amine and carboxyl terminated rubbers*

S. C. Kunz, J. A. Sayre and R. A. Assink
Sandia National Laboratories, Albuquerque, New Mexico 87185, USA
(*Received* 29 *March* 1982; *revised* 10 *May* 1982)

The morphology (dispersed phase composition, size distribution, and particle/matrix interface shapes) of epoxy resins modified with 5–15 parts by weight (pbw) of carboxyl (CTBN) and amine (ATBN) terminated butadiene acrylonitrile rubber have been characterized. The characterization techniques were transmission electron microscopy coupled with energy dispersive X-ray analysis, differential scanning calorimetry and proton and ^{13}C nuclear magnetic resonance. ATBN modified epoxies have a diffuse-appearing interface between the dispersed rubber phase and the epoxy matrix, in contrast to the sharp boundaries of CTBN particle interfaces. Interface mixing of epoxy and rubber, hypothesized initially to explain the interface diffuseness in ATBN modified epoxy, was not found in either CTBN or ATBN modified epoxy. The difference in interface appearance is attributed to ATBN particles having highly irregular shapes compared to the nearly spherical CTBN particles. Bimodal particle size distributions are observed with both modifiers. Both rubber modifiers also produce essentially identical toughness values which do not increase with rubber content in the range 5–15 pbw despite a commensurate increase in the population of large particles.

Keywords CTBN rubber; ATBN rubber; toughened epoxies; interface shape; particle size distribution

INTRODUCTION

Enhancing the toughness of epoxy resin by the addition of carboxyl-terminated butadiene acrylonitrile (CTBN) rubbers to produce a dispersed particulate phase has been widely documented in the past decade. In general, two parameters emerge from existing theories as critical to the toughening mechanism: volume fraction[1-3] and size distribution[4-6] of the rubber particles. In addition, rubber particle composition[3,7-11] and particle/matrix interface composition[6,10,11] have been suggested as significant in the toughening process. A definitive relationship between toughness and these structural parameters has not been established because of the difficulty in their measurement. Advances have been made in quantitative characterization of the morphology and phase composition of a CTBN rubber-modified epoxy[11]. Scanning transmission electron microscopy coupled with energy dispersive X-ray analysis, ^{1}H and ^{13}C nuclear magnetic resonance, and differential scanning calorimetry were used to characterize the particle/matrix interface shape and composition, volume fraction of the dispersed phase, and respective compositions of the matrix and rubber particles.

This paper compares the morphology and toughness of two types of rubber-toughened epoxies: a CTBN modified resin and the identical resin modified with an amine-terminated butadiene acrylonitrile (ATBN) rubber. The two systems were characterized using the analytical techniques described above. The toughness-morphology dependence is discussed in terms of the volume fraction and particle size distribution of the dispersed phase and the particle/matrix interface characteristics.

* This work performed at Sandia National Laboratories supported by the US Department of Energy under contract number DE-AC04-76-DP00789

EXPERIMENTAL

Materials

The epoxy resin used in all experiments was Epon 828, a diglycidal ether of bisphenol A with an average MW of 370 g mol^{-1}, produced by the Shell Chemical Company. The amine and carboxyl terminated rubbers, manufactured by B. F. Goodrich Chemical Company, are designated Hycar 1300X16 and 1300X8, respectively. These rubbers are random copolymers of butadiene and acrylonitrile containing 17% acrylonitrile. The amine terminated rubber is prepared by reacting the carboxyl-terminated rubber with *N*-aminoethylpiperazine. Thus except for the type of termination, the rubbers are the same. The carboxyl-terminated rubber has a density of 0.948 g cm^{-3}, and the amine-terminated rubber has a density of 0.956 g cm^{-1}. The number average molecular weight is 3300–3500 g mol^{-1} for both rubbers. A polyoxypropyleneamine, Jeffamine T-403, produced by the Jefferson Chemical Company was used as the curing agent. In addition, 2,4,6 tri(dimethylaminomethyl) phenol, DMP-30 (Shell Chemical Co.), was used to accelerate the curing reaction. The ratios of materials used are shown as parts by weight (pbw) in *Table 1*. The amount of curing agent was adjusted to keep a constant ratio of epoxy to amine groups as the amount of rubbermodifier was varied.

The ATBN- and CTBN-modified epoxies were prepared using two different processes. The more reactive amine terminated rubber was added directly to epoxy

0032-3861/82/131897-10$03.00

Table 1

Epoxy (pbw)	Carboxyl terminated rubber (1300X8) (pbw)	Amine terminated rubber (1300X16) (pbw)	T-403 curing agent (pbw)	DMP-30 catalyst (pbw)	Matrix glass transition temp. (°C)	Dispersed phase glass transition temp. (°C)
100	–	–	36	1	87.1	–
95	5	–	34	1	86.4	–58.1
90	10	–	32	1	86.1	–63.5
85	15	–	30	1	86.0	–62.9
95	–	5	33	1	87.3	–58.6
90	–	10	31	1	87.0	–63.2
85	–	15	29	1	86.6	–61.7

with curing agent and accelerator. The mixture was then cured for 16 h at 71 C. The less reactive carboxyl terminated rubber was first reacted with epoxy at 150 C for 3 h. The large molar excess of epoxy (100:1) in the pre-reaction caused the rubber to be essentially end-capped. Later this adduct was combined with curing agent and accelerator and cured for 16 h at 71 C. During the cure, both the ATBN and CTBN modified epoxies suddenly became cloudy 25 min after the addition of the curing agent and accelerator. Two minutes after the onset of cloudiness in both types of rubber-modified epoxies, gelation occurred.

Test specimens were machined from plates cast to a thickness of 12 mm. *Table 1* lists the glass transition temperatures (T_g) of the matrix and dispersed phases for each composition studied. The matrix and dispersed phase transition temperatures were measured at a heating rate of 20 C min^{-1} using a Perkin Elmer Differential Scanning Calorimeter Model DSC-2. The T_g was taken as the onset of the transition in a plot of heat capacity *versus* temperature. The change in heat capacity of the dispersed phase was measured below room temperature by recording the difference in heat capacity between a rubber-modified epoxy and an unmodified epoxy. This was accomplished by placing a rubber-modified epoxy sample in one d.s.c. sample holder and an unmodified epoxy sample in the other holder. The sample sizes were selected to give equal weights of epoxy in both samples. This procedure assumes that pure (unmodified) epoxy is a good model for the matrix in the rubber-modified epoxies; results of this study and previous work[11] indicate that this is a good assumption. Above room temperature the reference sample holder pan was left empty allowing measurement of changes in heat capacity of the entire sample.

Transmission electron microscopy (TEM)

Width of the dispersed-phase/matrix interface as well as volume fraction and particle size were determined using *TEM*. Samples machined into 7.7 mm rods from the cast plates were stained for ten minutes in a tetrahydrofuran solution containing 1% osmium tetroxide, as suggested by Riew and Smith[12] for enhancing contrast between the particles and the matrix. Ultra-thin sections of the stained material were obtained using a Porter-Blum MT-2-B Ultra Microtome with a diamond knife at an inclined angle of 45 . Specimens were microtomed to a 100 nm thickness to minimize effects of sample thickness.

The microscopy studies were done using a JEOL 100C scanning transmission electron microscope equipped with a KEVEX 5100 spectrometer for energy dispersive X-ray analysis. This combination allowed the variation in osmium concentration throughout the dispersed phase and the matrix to be investigated. An 18 nm electron beam was used in order to minimize the area being examined for each measurement. Since the X-ray detector is located on an axis perpendicular to the beam axis, the samples were rotated 45 from the plane perpendicular to the beam to increase the signal received by the X-ray detector. The $M\alpha$ osmium peak height was used as a measure of relative osmium concentration. Osmium reacts selectively with the butadiene in the rubber[13], and therefore a direct correlation exists between the osmium concentration and the rubber concentration.

Measurements at the epoxy–rubber interface are complicated by the fact that the dispersed phase is present as spherical particles. After microtoming, the epoxy rubber interface retains the curvature present in the bulk sample. For a 1 μm particle diameter and a 100 nm slice thickness, the departure from a straight line at the interface is less than 10 nm. This was considered a second order effect for all systems of both modifiers studied. Because of this small departure, the microtomed rubber particles were treated as right circular cylinders. After rotation the particle images are elliptical. Measurement of the osmium concentration was done along the major axis of the ellipse to avoid sampling through the overlapping epoxy–rubber layer formed by tilting the sample. The sampling location was made apparent by a contamination spot left on the specimen by the electron beam. A typical photomicrograph of a particle that has been analysed for osmium is shown in *Figure 1*. The carbon buildup on the specimen surface at the point being analysed, together with beam scatter in the sample were estimated to broaden the 18 nm electron beam to 50 nm[14].

Photomicrographs were taken at a magnification of 10 000X for determination of volume fraction and size of the dispersed phase. *Figure 2* shows a photomicrograph, enlarged to a magnification of 20 000X, for each of the six rubber-modified epoxies studied. Random areas from the photomicrographs containing between 200 and 400 particles were scanned with a Cambridge-Imanco Quantimet 720 image analysis computer system. The particle volume fractions were approximated by the measured area fraction, and the observed distributions of particle sizes (diameters) were converted to true particle size distributions using the method described below. Due to insufficient contrast between particles and surrounding matrix (see *Figure 1*) it was necessary to manually encircle the particles in the photomicrographs prior to scanning by the Quantimet. This procedure was straightforward for the CTBN modified epoxy except for the difficulty in

accurately detecting and encircling particles less than 20 nm in diameter. However, for the ATBN modified material, where the boundary between particle and matrix appears noticeably less defined, the determination of discrete rubber particles was more subjective.

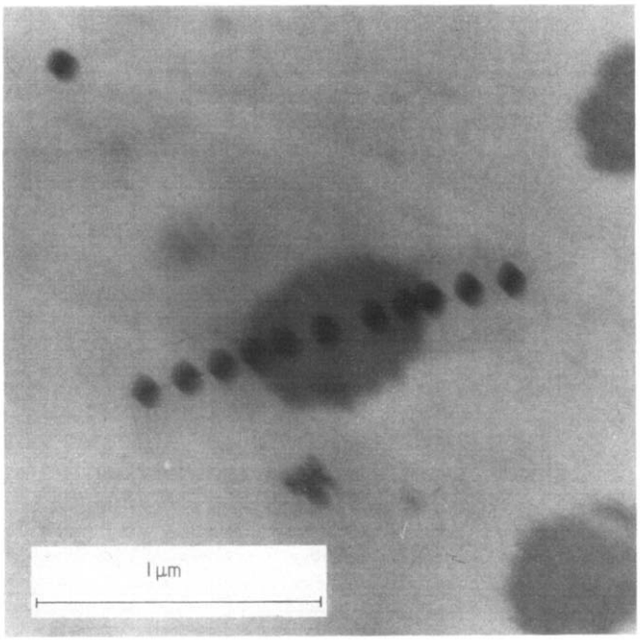

Figure 1 Transmission electron photomicrograph of rubber-modified epoxy at 40 000X magnification showing sampling location for energy dispersive X-ray analysis and electron beam contamination spots

The observed distribution of particles was treated as a set of non-overlapping spherical particles from a thin section of thickness t with a frequency distribution $g(x)$. This is related to the true frequency distribution, $f(x)$, by the following Abel-type integral equation[15]:

$$g(x) = c_1 f(x) + c_2 x \int_x^u \frac{f(y)}{\sqrt{y^2 - x^2}} \, dy \qquad (1)$$

where $c_1 = \frac{t}{t+m}$, $c_2 = \frac{1}{t+m}$ and $m = \int_0^u y f(y) dy$

This equation was solved analytically by Amos and Davis[15]. The data obtained in this study were fit by Amos and Davis to give $g(x)$ using a least squares spline fit. In this fit, $g(x)$ was constrained so that $f(x)$ would be non-negative over the range of interest.

Nuclear magnetic resonance (n.m.r.)

The ^1H measurements were made on a Bruker SXP spectrometer operating at 100 MHz in the phase sensitive detection mode. The ^{13}C spectra were taken on a system consisting of the Bruker SXP spectrometer operating at 25.16 MHz, a Varian XL-100 spin decoupler operating at 100.1 MHz in the broadband mode and a laboratory built probe. The ^1H measurements were performed over a range of temperature while all ^{13}C measurements were performed at 40 C.

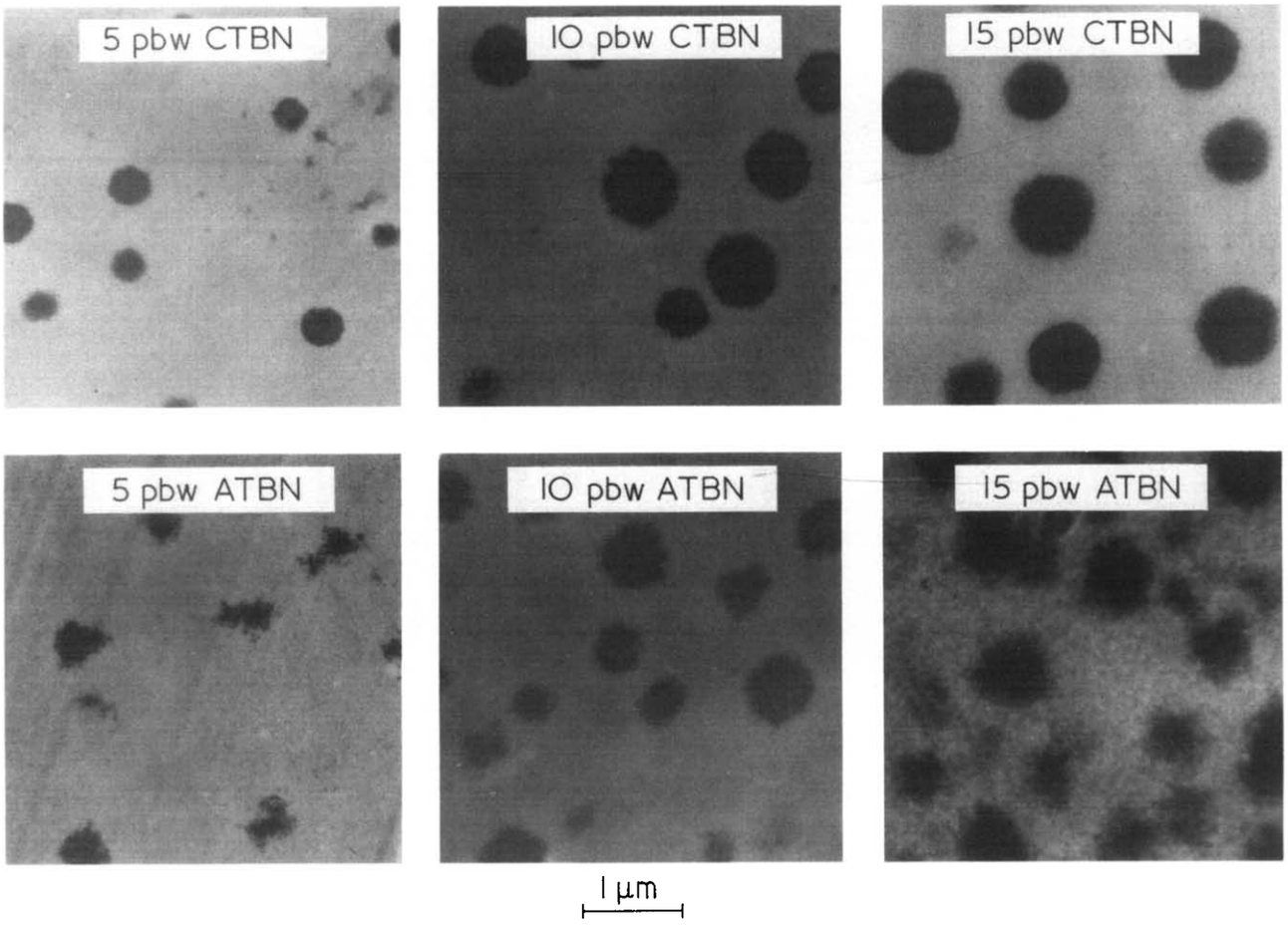

Figure 2 Transmission electron photomicrographs of osmium-stained CTBN and ATBN modified epoxy at 20 000X magnification

Table 2

	Weight fraction of rubber W_R (%)	Volume fraction of rubber V_R (%)	Volume fraction of particles V_P (%)	Volume fraction of mobile phase (±2%)
CTBN	3.70	4.48	8.0 ± 1.9	4.8
	7.52	9.03	13.4 ± 4.1	8.8
	11.45	13.62	21.5 ± 5.8	12.3
ATBN	3.73	4.48	7.9 ± 3.13	5.5
	7.58	9.03	15.0 ± 3.7	8.3
	11.54	13.64	29.1 ± 3.8	12.0

For a two-phase polymeric material in which one phase is above and the other phase is below their respective glass transition temperatures, the ^{1}H magnetization is composed of fast- and slow-decaying components[16]. The relaxation behaviour is governed by perturbations in the local magnetic field caused by neighbouring nuclear dipoles. If the polymer segments are rigid, the nuclei experience the full effect of these interactions and the relaxation process is rapid. The free induction decay of such a material can be approximated by a Gaussian function:

$$M(t) = M_0 \exp(-t^2 M_2/2) \tag{2}$$

where M_0 is the initial magnetization and M_2 is the second moment of the resonance line in the frequency domain. If the polymer segments are undergoing rotational and/or translational motions, the interaction fluctuates and begins to approach an average value of zero during the time span of an experiment. This is referred to as motional narrowing and causes the relaxation time of the magnetization to increase. The decay for segments above their glass transition temperature can be written:

$$M(t) = M_0 \exp(-t/T_2) \tag{3}$$

where T_2, the spin–spin relaxation time, increases with increasing segmental mobility. A linear combination of these decay functions, equations (2) and (3), was used to provide a nonlinear least squares fit of the ^{1}H free induction decays. The pre-exponential coefficients of the two terms were then proportional to the number of hydrogens in the rigid and mobile phases respectively. The root-mean-square deviation of the experimental points from the theoretical fit was consistently less than 0.5% of the initial magnetization. The magnitude of the free induction decay extrapolated to time zero was within 2% of the initial magnitude of the slowly decaying free induction signal of the uncured material when compared on an equal weight basis. These facts imply that the decomposition is accurate to within 2%.

The ^{13}C Fourier transform spectra were taken under low power decoupling conditions which eliminated only the scalar component of the dipole dipole interaction. The intensities of the broad lines from the rigid phase were very low and could not be distinguished from baseline noise because the areas under each line, whether broad or narrow, were approximately equal to the number of carbons contributing to the peak. Thus the composition of the mobile phase could be determined by analysing the intensities and positions of the well-defined motionally narrowed peaks.

Mechanical properties

Fracture toughness, K_{Ic}, was measured from three-point bend tests on machined single edge-notched (SEN) specimens of 6.4 mm width (t), 12.7 mm depth (w) and 76.2 mm length. A shallow notch ($\leqslant 0.5$ mm) was cut into one edge, across the thickness of a sample, and a sharp pre-crack was formed (~ 3 mm) by tapping a razor blade into the notch. The specimens were tested in an opening mode at 0.25 cm min^{-1} using a span-to-depth (S/w) ratio of 4. K_{Ic} was calculated using the Irwin relation applicable to the geometry and loading configuration of a SEN specimen with crack length a[16]:

$$K_{Ic} = Y\sigma\sqrt{a} = Y\frac{6M}{tw^2}\sqrt{a} \tag{4}$$

M is the bending moment equal to $PS/4$ where P is the load at fracture, and Y is a geometrical factor calculated from the ratio a/w. Ten determinations were made for each of the pure resin and rubber-modified materials.

Measurement of the elastic modulus, E, was done according to method D790 of the American Society for Testing and Materials (ASTM) on flat rectangular bars. The machined specimen dimensions were 6.4 mm × 12.7 mm × 127 mm (depth × width × length). Load was applied within the linear load-deflection range at 0.25 cm min^{-1}. Calculations of true elastic modulus of all specimens in flexure were made after correcting measured compliances for machine compliance contributions.

Unnotched fracture strengths of both pure and rubber-modified resin were measured in tension according to ASTM method D638. Machined specimens were tested at 0.5 cm min^{-1} until fracture occurred. The fracture load typically coincided with the maximum sustainable load (i.e., no softening) after relatively uniform and extensive elongation of the guage section.

RESULTS

Volume fraction of dispersed phase

The total volume fraction of rubber, V_R, which would appear as precipitated particles assuming that none of it remains in solution with the epoxy, is given by:

$$V_R = \frac{W_R/\rho_R}{W_E/\rho_E + W_R/\rho_R} \tag{5}$$

where W_R and W_E are the weight fractions of rubber and epoxy. The density of epoxy resin was measured as 1.157 g cm^{-3}; that of CTBN and ATBN rubber is 0.948 and 0.956 g cm^{-3}, respectively. Calculated values of V_R are shown in *Table 2* for comparison with the particle volume fractions, V_P, obtained by the *TEM* and ^{1}H n.m.r. techniques.

The per cent rigid hydrogen determined by decomposition of the free induction decay for the CTBN and ATBN modified epoxies are shown as a function of temperature in *Figure 3*. Since both phases of the material were becoming rigid below 0°C, the free induction decays were difficult to fit to a two component decay. Above 80°C the matrix phase was becoming mobile and above 100°C the decays were difficult to fit. Between 0° and 80°C the dispersed phase was mobile and the matrix phase was rigid. The characteristic frequency of this technique is near 10^4 Hz so the transitions occur at higher temperatures

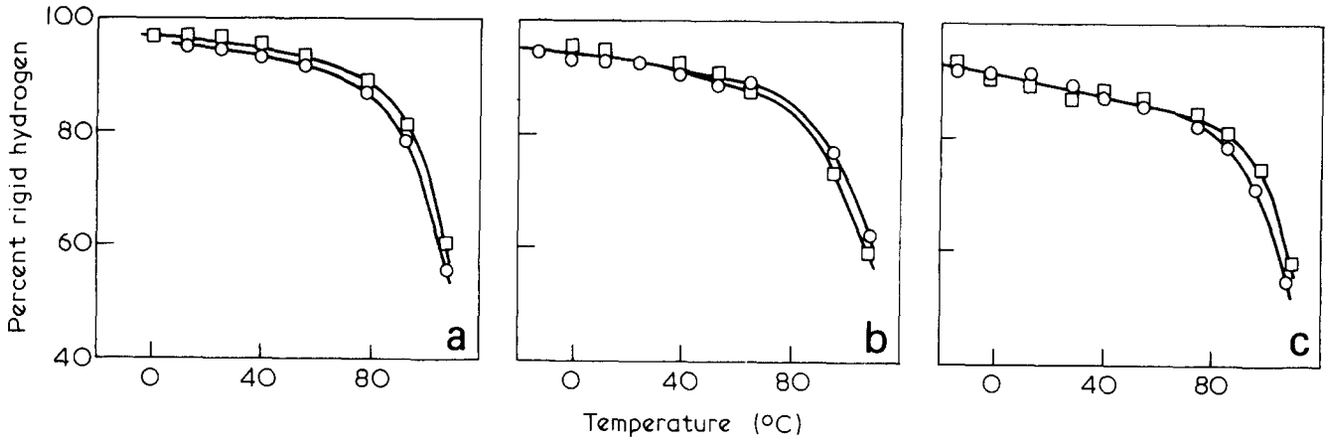

Figure 3 Immobile hydrogen content as a function of temperature for (a) 5pbw; 9b0 10 pbw; (c) 15 pbw of CTBN and ATBN rubber in epoxy resin. ○ ATBN; □ CTBN

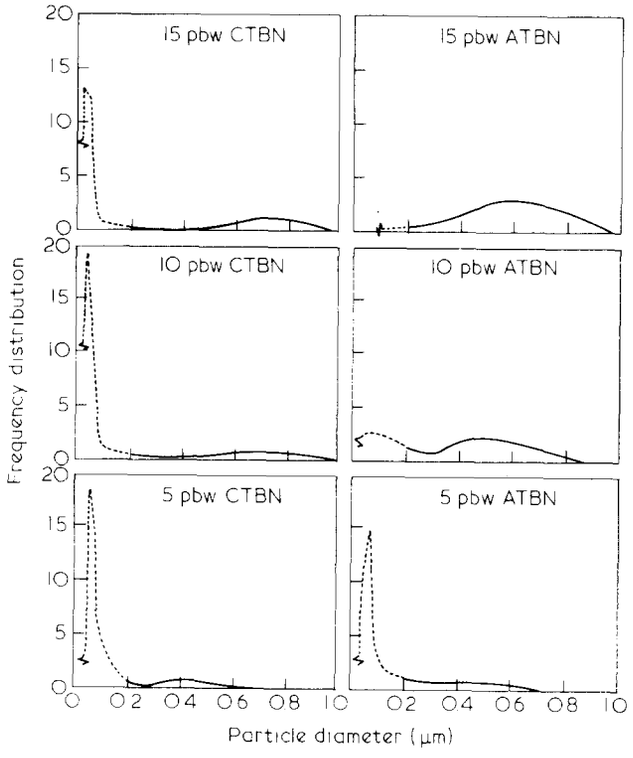

Figure 4 Bimodal distribution of particle sizes in CTBN and ATBN rubber modified epoxy. The populations of small particles indicated by the dotted lines underestimate the true distributions

compared to those measured by low frequency methods such as differential scanning calorimetry. Since the per cent rigid hydrogens was decreasing slowly between 0 and 80 C the midpoint at 40 C was chosen to compare experimentally determined per cent mobile hydrogens of CTBN and ATBN modified epoxy. The per cents of mobile hydrogens were converted to volume fraction of mobile phase by consideration of each components' molecular formula and density. The results are shown in *Table 2*. Within experimental error, the expected content of mobile phase is observed for each material.

Distribution of particle size

The frequency distributions of rubber particle sizes obtained using equation 1 are plotted in *Figure 4*. These illustrate a distinct bimodal distribution of particle sizes in both ATBN and CTBN rubber modified epoxies. Also apparent is a marked increase in the number of large

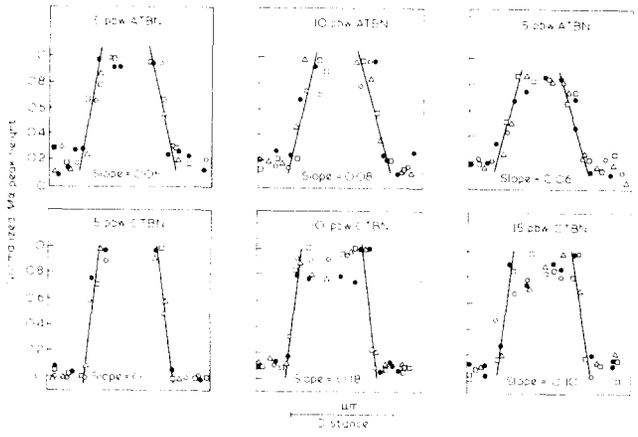

Figure 5 Variation of osmium concentration through the dispersed phases in ATBN and CTBN rubber modified epoxy. Each symbol represents a separate particle. Calculated values are given for the apparent concentration gradients at the interfaces

particles (> 200 nm) as the rubber content increases. The distribution of small particles is inaccurate and does not represent the true distribution due to the difficulty noted earlier in visually identifying small particles from the photomicrographs (*Figure 2*).

Interface shape

Measurement of osmium concentration along a line through the centre of a particle gives information about the shape of the interface between the dispersed rubber phase and the epoxy matrix. Since the sampling-electron beam is up to 50 nm in diameter as it passes through a sample, the changes in concentration are measured in discrete steps through the interface. *Figure 5* gives apparent interface concentration profiles of the amine and carboxyl terminated rubber-modified epoxies at the three rubber concentrations studied. These profiles are a compilation of measurements from four particles for each system. To compensate for differences in particle diameters, the apparent (visual) interface of each particle was used as a reference point, and the osmium concentration was plotted as a function of distance from it. A least-squares regression was used to obtain the slopes of lines best fitted to each profile. These slope values, shown in *Figure 5*, support observations from *TEM* photomicrographs that amine terminated rubbers produce a more diffuse matrix boundary than carboxyl terminated rubbers at a given concentration.

Table 3 The spin–spin relaxation times of the slowly decaying portions of the ^1H free induction decays. All values are ±5%

Rubber modified epoxy (pbw rubber)		T_2 (μs) 26°C	T_2 (μs) 60°C
CTBN	5	360	431
	10	353	459
	15	350	452
ATBN	5	282	318
	10	265	362
	15	280	351

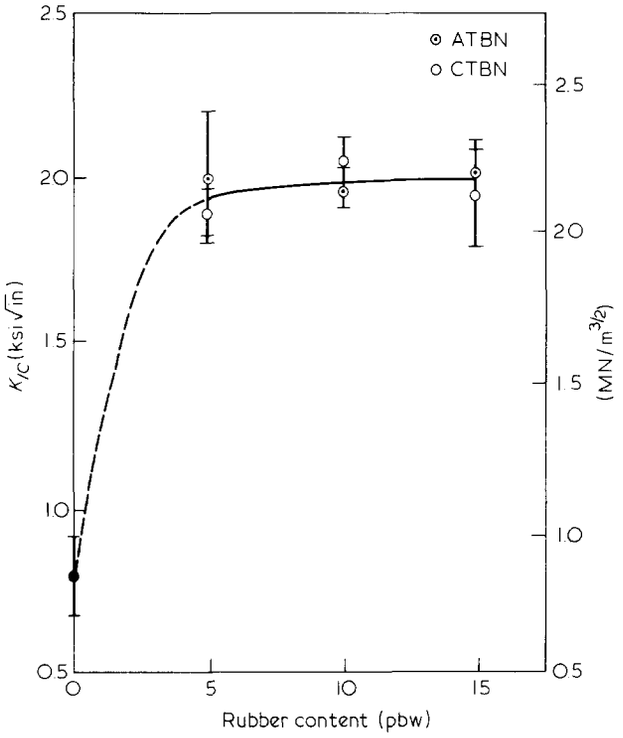

Figure 6 Fracture toughness as a function of ATBN and CTBN rubber concentration in epoxy

Significant segmental mixing between phases would result in an observed glass transition at a temperature, or temperatures, intermediate to the pure epoxy and pure rubber transitions. The lower temperature transition in *Figures 3(a), (b)* and *(c)* is impossible to determine precisely by ^1H resonance because as the dispersed phase begins to immobilize, the free induction decay becomes increasingly difficult to fit. However, the Figures show that the upper temperature transition occurs at the same temperature regardless of the kind or amount of rubber phase present. The d.s.c. results in *Table 1* show no change in either transition temperature giving further evidence of complete separation.

Table 3 contains the spin–spin relaxation times, T_2, of the slowly decaying portion of the ^1H free induction decay. T_2 which increases with increasing mobility, is seen to be independent of the amount of rubber present. However, the mobility of the dispersed phases in the CTBN modified materials is consistently greater than the mobility of the dispersed phases in the ATBN modified materials. ^{13}C Fourier transform spectra under low power decoupling conditions were recorded for the 10 and 15 pbw rubber samples to determine if any of the epoxy segments were mobile. Mobile epoxy segments should be observed if these segments were dissolved in the dispersed phase or if the interface were extremely broad. Comparison of these spectra with the spectrum of a model compound discussed in an earlier paper[11] shows no peaks corresponding to mobile epoxy carbons.

Fracture toughness

Calculated K_{Ic} values are plotted as a function of rubber content in *Figure 6*. The lowest concentrations of both ATBN and CTBN rubber produce a near 2.5-fold increase in fracture toughness. However, further increases in either rubber have little effect on fracture toughness enhancement. This behaviour is noteworthy in that it is atypical of trends observed in other epoxy/curing agent systems modified with the same CTBN rubber[1–6,9,10].

The critical strain energy release rate, G_{Ic}, also known as toughness, was calculated from the measured values of K_{Ic} and elastic bending modulus, E, according to the Irwin relation[18] for linear elastic fracture mechanics:

$$G_{Ic} = \frac{K_{Ic}^2}{E} \tag{6}$$

Figure 7 illustrates the decrease in stiffness of modified epoxy with increasing rubber content. The toughness values for both rubber modified systems plotted in *Figure 8* show only a slight variation with rubber content in the range 5–15 pbw. The greater than five fold improvement in G_{Ic} over that of pure epoxy, observed for 5 pbw of CTBN and ATBN rubber, increases to a seven fold toughness enhancement for 15 pbw.

Figure 9 shows the variation of unnotched tensile strength with rubber concentration. As noted previously, little difference is seen between the two rubber systems, and the strength decreases also follow a rule-of-mixtures dependence on rubber concentration.

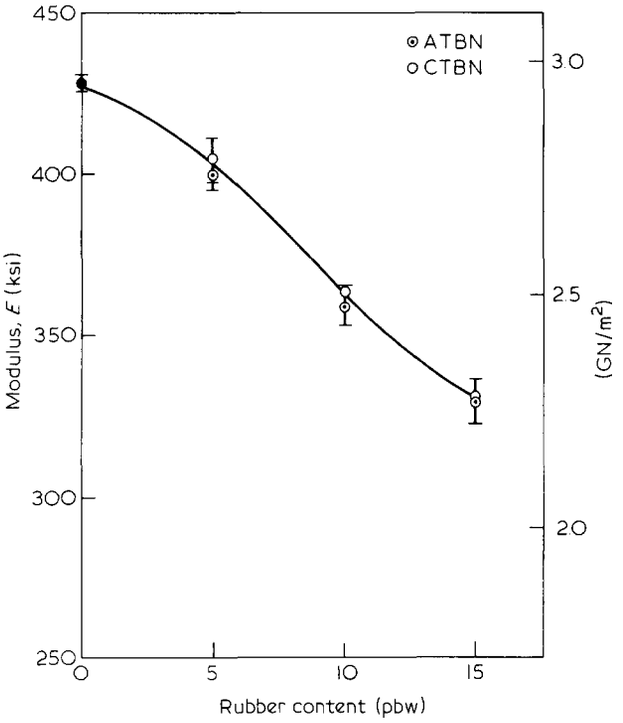

Figure 7 Flexural stiffness dependence of ATBN and CTBN modified epoxy on rubber content

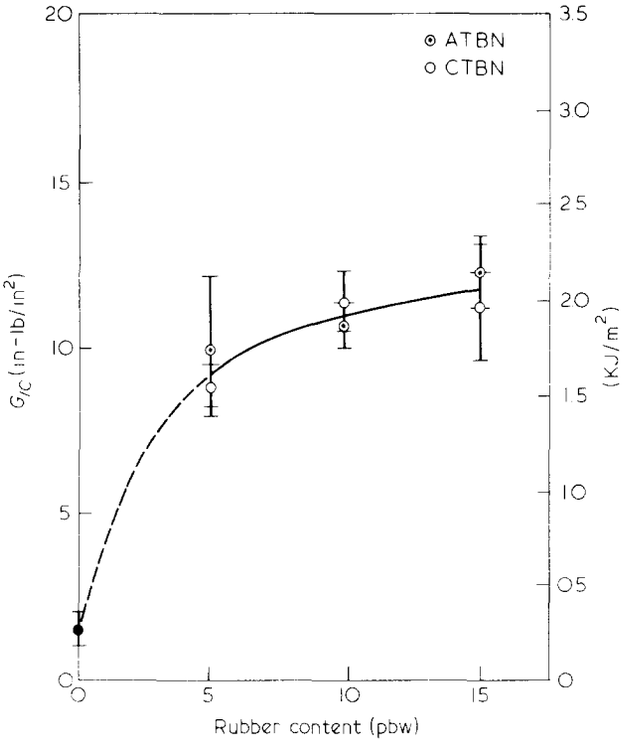

Figure 8 Toughness dependence of ATBN and CTBN modified epoxy on rubber concentration

DISCUSSION

Investigation of the toughness morphology dependence of ATBN-modified epoxy was motivated by initial *TEM* observations of its two phase microstructure. The diffuse boundary between the dispersed and matrix phases, peculiar to the ATBN material, suggested a source for enhanced energy dissipation during fracture, e.g., by viscoelastic deformation or tearing. The visually diffuse interface was thought to indicate segmental mixing of rubber and epoxy between the two phases which would provide an interphase region with a continuously varying relaxation spectrum. If a continuously varying concentration gradient of rubber in solution with epoxy is assumed, this interphase would provide a toughening mechanism operable over a range of temperatures and frequencies (strain rates).

Results of the interfacial characterization and toughness measurements presented in this study do not reveal the anticipated interphase region nor a toughness improvement over CTBN-modified epoxy. Although proton n.m.r. and transmission electron microscopy do not unambiguously exclude a variable rubber concentration interphase, the ^{13}C n.m.r. and differential scanning calorimetry data give direct evidence against segmental mixing. The volume fraction of dispersed phase in either rubber-modified system has little effect on toughness, contrary to expectation. The parameter which differs most significantly between CTBN and ATBN modified epoxy, but yet does not affect the toughness, particle shape, is discussed in detail below.

Particle shape

The transmission electron micrographs in *Figure 2* illustrate clearly the primary morphological difference between particles in CTBN and ATBN modified epoxy. For all three concentrations, the essentially circular cross-sections of CTBN particles are indications of a near spherical shape. In contrast, ATBN particles show highly irregular contours which often appear as agglomerated islands of smaller particles. The initial interpretation of the ATBN particle boundaries was that of a broad, variable-concentration interface between rubber and epoxy phases. However, the ^{13}C n.m.r. results show very little mobile epoxy present in both the amine and carboxyl terminated rubber modified epoxies. The mobile hydrogen concentrations of the two systems have similar temperature dependencies in the temperature range between the pure phase transitions (*Figure 3*). This indicates that there is no appreciable difference in the amount of inter-phase mixing between the ATBN and the CTBN materials. Differential scanning calorimetry measurements also show no indication of greater phase mixing of the ATBN-epoxy. The locations and widths of the transitions are the same for both rubber modifiers studied. All these results point to the conclusion that any epoxy present in the dispersed phase is precipitated as glassy epoxy.

The reason for the difference in particle shape is not understood. Originally it was speculated that differences in solubility caused precipitation to occur at different times in the epoxy cure. But visual observation of the epoxy cure revealed that both rubber-modified epoxies become cloudy at the same time. While becoming cloudy is not a definitive test for precipitation, the test does suggest that there is no appreciable solubility difference between the CTBN and ATBN rubbers. This is further supported by the process used to make these rubbers (ATBN is made directly from CTBN). The compositions and molecular weights differ only by the *N*-aminoethylpiperazine used to form the amine termination of ATBN rubber. Lee and Neville[20] report that primary amines react with epoxy twice as fast as secondary amines. The reaction between epoxy-endcapped CTBN and T-403, a primary amine, will be faster therefore than the reaction between ATBN, a secondary amine, and epoxy. Speculatively, this would result in larger epoxy networks being formed on the ends of CTBN molecules influencing in turn particle shape and size.

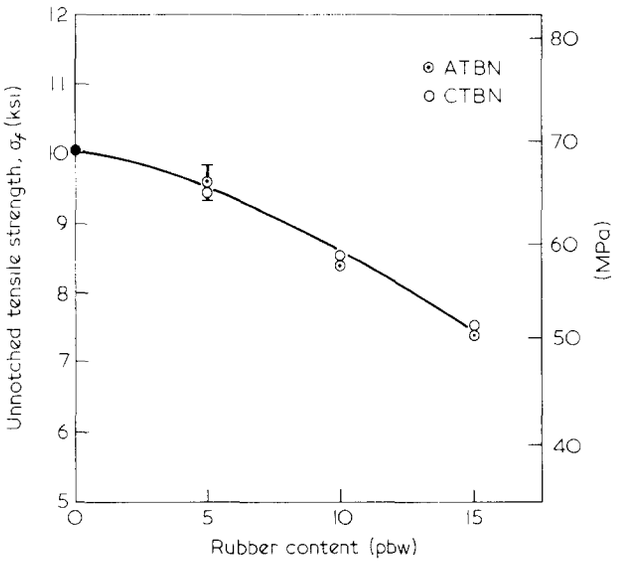

Figure 9 Fracture strength as a function of ATBN and CTBN rubber concentration in epoxy

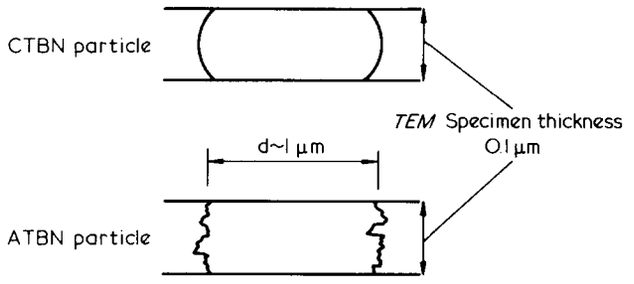

Figure 10 Schematic comparison of CTBN and ATBN particle surfaces as detected by an electron beam in energy dispersive X-ray analysis for measurement of interface composition. The direction of the electron beam is vertical in the plane of the Figure

Differences in surface irregularity between ATBN and CTBN particles affect interface composition measurements, as illustrated schematically in *Figure 10*. When traversing from the matrix to an idealized CTBN particle (a), the electron beam detects an abrupt transition in rubber content (as measured by changes in osmium concentration). In the case of a simulated ATBN particle (b), the variable amount of particle being sampled, especially near particle edges, results in a more gradual increase in rubber concentration. This explains how the interface concentration gradients of CTBN modified epoxies can appear approximately twice as sharp as the ATBN material (*Figure 5*). Thus, apparent interface diffuseness is concluded to reflect particle irregularity rather than breadth of an interphase.

Particle surface irregularity also results in greater surface area for an equivalent particle volume on a microscopic scale. The greater surface area afforded by irregular boundaries of ATBN particles, compared to the nearly spherical rubber particles of CTBN modified epoxy, leads to greater contact between rubber segments and neighbouring immobile epoxy segments. This interaction between phases could account for the reduction in mobility of the amine terminated rubber segments indicated by the T_2 measurements in *Table 3*. Analogous behaviour was observed by L. W. Jelinski *et al.* who measured the ^{13}C linewidth of the mobile aliphatic carbons of several polyester elastomers[19]. They concluded that the increase in linewidth with hard block content was caused by a restriction in the motion of aliphatic carbons directly attached to the hard segments.

Effects of particle shape are not addressed by existing theories for the increased toughness of CTBN modified epoxies, probably due to the vast numbers of studies dealing only with uniform, spherical particles. Apart from particle-matrix bonding and stress concentration effects, the role of particle shape in toughening mechanisms such as matrix deformation (crazing, shear banding) or tear energy of the rubber particles is not immediately obvious. The scanning electron photomicrographs of fracture surfaces from ATBN and CTBN modified epoxy in *Figure 11* show marked differences. All three concentrations of CTBN modified epoxy have deep rubber-lined cavities which, based on previous observations[3], are a result of failure by tear propagation in highly strained rubber particles. The tear paths in both 5 and 10 pbw ATBN modified epoxy are much more shallow and, in the 15 pbw material, nearly coincide with the principal fracture plane. This difference in fracture mode cannot be attributed to differences in particle size, as in a previous study[3], since the particle sizes of the two systems in this study are effectively identical. It is possible that the surface irregularity of ATBN particles, evident in the fractographs, acts as stress-concentrating defects which initiate low-strain tear failure giving rise to flat fracture surfaces.

Particle volume fraction

The volume fractions of dispersed phase obtained from transmission electron photomicrographs are nearly double those predicted based on the amount of rubber added, as shown in *Table 2*, for both CTBN and ATBN modified epoxy. Nuclear magnetic resonance measurements of the mobile hydrogen concentration indicate, however, that the amounts of mobile material present approximately equal the amounts of rubber added. This means that either the dispersed phase contains epoxy, which must be immobile, or that measurement of particle volume fraction from *TEM* photomicrographs leads to significant errors.

Several sources of error have been identified in measuring particle fraction from *TEM* photomicrographs. As pointed out previously[11], a finite slice thickness inherently leads to overestimation of the volume fraction. In addition, diffuse appearance and poor contrast make definition of particle boundaries very difficult. Encircling the particles by hand for Quantimet measurement introduces error which is probably considerable for ATBN particles due to their irregular shape. In addition, particles less than 10 nm in diameter were not included in the particle count. Taking these particles into account would led to still higher volume fractions. The magnitude of these errors could not be determined, but it is thought that they cannot account entirely for the difference between measured volume fraction of particles shown in *Table 2* and amount of rubber added. Instead, a major contribution to the volume fraction of dispersed phase is thought to result from immobile epoxy. Reaction between the rubber end groups and epoxy monomer necessarily leads to presence of epoxy in the rubber phase because many particle diameters are much greater than the mean end-to-end distance of the rubber molecules ($\approx$10 nm). Since these epoxies were not found to be mobile, they must be present as glassy hard segments. These segments are not visible in the *TEM* sections indicating that they are smaller than the sections thickness of 100 nm. Since it was not possible to estimate the magnitude of error introduced in the particle volume fraction measurement, the amount of immobile epoxy present in the dispersed phase cannot be quantitatively assessed with the techniques used in this investigation.

Particle size distribution

No conclusive studies have elucidated the dependence of toughness on particle size and, more importantly, particle size distribution (e.g., bimodal), and current theories differ in their predictions. The work of Sultan and McGarry[4], suggests that large (0.1–1 μm) particles cause crazing and are five times more effective toughening than shear band producing small (0.01 μm) ones. In contrast, a rubber particle tear energy model[3] predicts no substantial size dependence when the particles are less than 1 μm but predicts a decrease in toughness for larger particle sizes.

The least expected and understood result obtained in this study is the absence of a dependence of toughness on

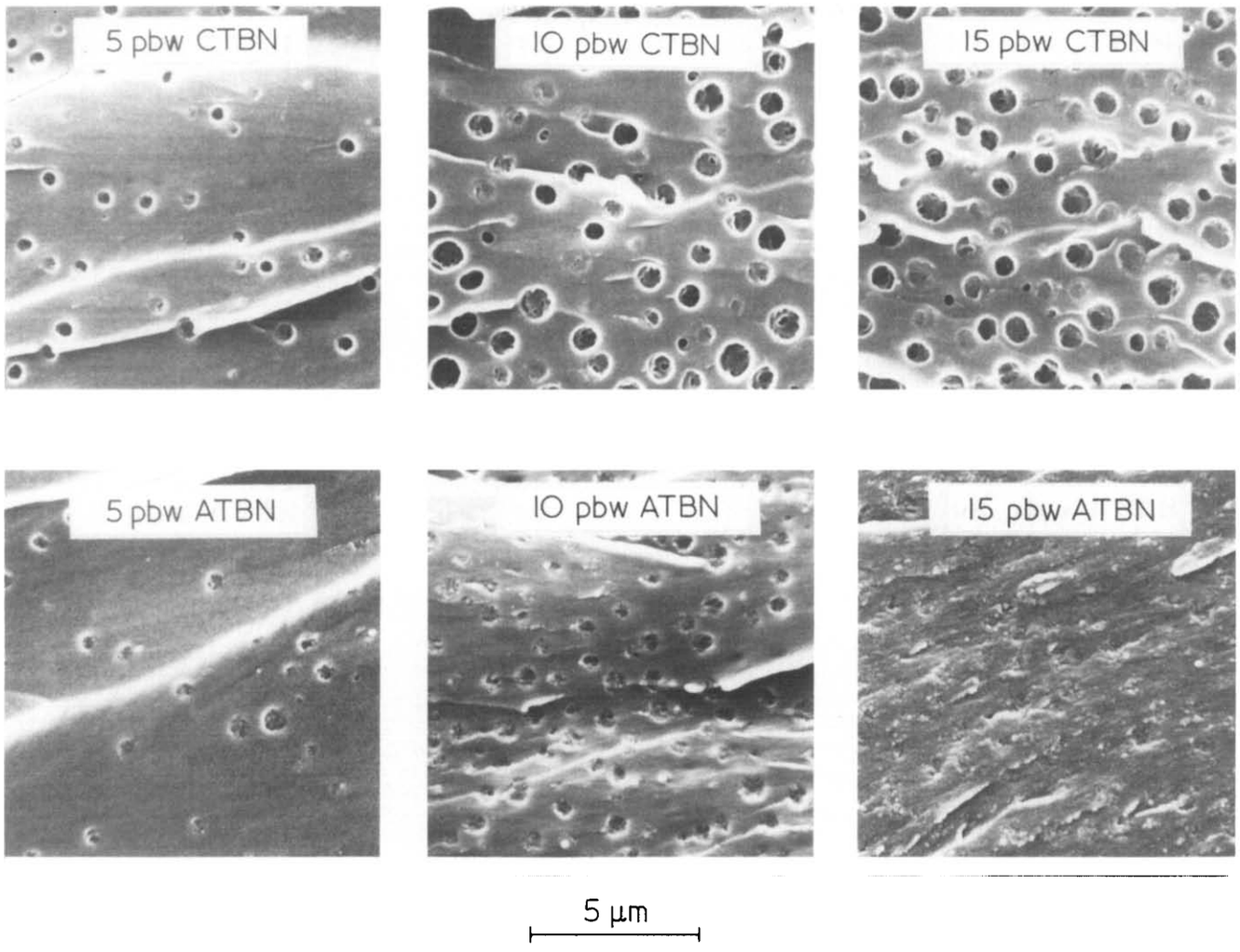

Figure 11 Scanning electron photomicrographs taken from fracture surfaces of CTBN and ATBN modified epoxy resin at 5000X magnification

particle volume fraction (*Figures 6* and *8*). CTBN-modified epoxies typically increase, sometimes linearly, with increasing rubber content[1-6]. In this study, the populations of large particles do increase with increasing amounts of both the CTBN and ATBN rubber modifier contents (*Figure 4*), but these are not accompanied by a significant change in K_{Ic} or G_{Ic}. This suggests that toughening is not enhanced by large particles. Instead, toughness may be dependent on the concentration of small particles which, unfortunately, could not be conclusively determined by the techniques used in this study.

CONCLUSIONS

Transmission electron microscopy suggests the presence of a gradually changing rubber concentration at the dispersed phase/matrix interface in ATBN modified epoxy, and a sharp interface in CTBN modified epoxy. However, ^{1}H and ^{13}C n.m.r. results together with d.s.c. data indicate that segmental mixing does not occur in either of the rubber modified epoxy systems studied. The diffuse appearance of the ATBN modified epoxy interface is attributed to an irregular particle shape which, unexpectedly, produces the same toughness as the more spherically shaped particles in CTBN modified epoxies. Toughness appears to be insensitive to changes in the large particle (0.2–1 μm) population for rubber concentrations between 5 and 15 pbw. This suggests that distribution of rubber particle sizes is more critical than overall volume fraction of particles to the toughness of rubber-modified epoxies.

ACKNOWLEDGEMENTS

Scanning transmission electron photomicrographs and energy dispersive X-ray spectra were taken by W. R. Sorenson. Quantimet analysis was done by K. S. Varga, and D. H. Huskisson took the scanning electron fractographs. J. E. Reich performed the differential scanning calorimetry measurements.

REFERENCES

1 McGarry, F. J., Willner, A. M. and Sultan, J. N. Research Report R69-59, Massachusetts Institute of Technology (1969)
2 Bucknall, C. B. and Yoshii, T. 'Third International Conference on Deformation Yield and Fracture of Polymers', PRI, Paper 13, Churchill College, Cambridge, April 1976
3 Kunz-Douglass, S., Beaumont, P. W. R. and Ashby, M. F. *J. Mater. Sci.* 1980, **15**, 1109
4 Sultan, J. N. and McGarry, F. J. *J. Polym. Eng. Sci.* 1973, **13**, 29
5 Rowe, E. H. and Riew, C. K. *Plast. Eng.* 1975, **31**, 45

6 Riew, C. K., Rowe, E. H. and Siebert, A. R. *Adv. Chem. Ser. No. 154*, Am. Chem. Soc., 1976, p. 326
7 Kalfoglou, N. K. and Williams, H. L. *J. Appl. Polym. Sci.* 1973, **17**, 1377
8 Visconti, S. and Marchessault, R. H. *Macromolecules* 1974, **7**, 913
9 Meeks, A. C. *Polymer* 1974, **15**, 675
10 Siebert, A. R. and Riew, C. K. 'The Chemistry of Rubber Toughened Epoxy Resins I', 161st Am. Chem. Soc. Mtg., Organic Coatings Plastic Div., Los Angeles, March 1971, p. 552
11 Sayre, J. A., Assink, R. A. and Lagasse, R. R. *Polymer* 1981, **22**, 87
12 Riew, C. K. and Smith, R. W. *J. Polym. Sci. A-1* 1971, **9**, 2739
13 Kato, K. *J. Elect. Microsc.* 1965, **14**, 220
14 Goldstein, J. I. and Yakowitz, H. 'Practical Scanning Electron Microscopy', Plenum Press, New York, 1975, p. 473
15 Amos, D. E. and Davis, J. A. 'Estimation of Particle Size Distributions', Sandia National Laboratories Report SAND 82-0511, Albuquerque, NM, 1982
16 Assink, R. A. and Wilkes, G. L. *J. Polym. Eng. Sci.* 1977, **17**, 606
17 Brown, W. F. and Strawley, J. E. *Am. Soc. for Test. and Mat., Spec. Techn. Pub. No. 381* 1965, p. 13
18 Irwin, G. R. 'Fracture', Encyclopedia of Physics, **6**, Springer, Berlin, 1958
19 Jelinski, L. W., Schilling, F. C. and Bovey, F. A. *Macromolecules* 1981, **14**, 581
20 Lee, H. and Neville, K. 'Hand book of Epoxy Resins' McGraw Hill, 1967, p. 5